Fourier Transform Techniques☆

Peter F Bernath, Old Dominion University, Norfolk, VA, United States

Introduction

The Fourier transform is ubiquitous in science and engineering. For example, it finds application in the solution of equations for the flow of heat, for the diffraction of electromagnetic radiation and for the analysis of electrical circuits. The concept of the Fourier transform lies at the core of modern electrical engineering, and is a unifying concept that connects seemingly different fields. The availability of user-friendly commercial computer programs such as IDL^{tm}, Maple^{tm}, Mathematica^{tm}, and Matlab^{tm} allows the Fourier transform to be part of every technical person's toolbox. The Fourier transform can be used to interpolate functions and to smooth signals. For example, in the processing of pixelated images, the high spatial frequency edges of pixels can easily be removed with the aid of a two-dimensional Fourier transform. This article, however, is not about the use of the Fourier transform as a tool in applied mathematics, but as the basis for techniques of analytical measurement.

Fourier's Integral Theorem

Fourier's integral theorem is a remarkable result:

$$F(\nu) = \int_{-\infty}^{\infty} f(t) e^{-i2\pi\nu t} dt \tag{1}$$

and

$$f(t) = \int_{-\infty}^{\infty} F(\nu) e^{+i2\pi\nu t} d\nu \tag{2}$$

where $F(\nu)$ is the Fourier transform of an arbitrary time-varying function $f(t)$, and $i = \sqrt{-1}$. We adopt the notation of lower case letters for a function, $f(t)$, in the time domain and upper case letters for the corresponding Fourier-transformed function, $F(\nu)$, in the frequency domain. The variable ν is the frequency in units of hertz (s^{-1}). The second Eq. (2) defines the inverse Fourier transform that yields the original function, $f(t)$. Eqs. (1) and (2) can be written in many ways, but the version above is convenient for practical work because of the absence of factors (e.g., $1/2\pi$) in front of the integrals. These factors can be an annoying source of errors in the computation of Fourier transforms. The variables t and ν can be replaced by any reciprocal pair (e.g., x, in cm, for optical path difference and $\tilde{\nu}$, in cm^{-1}, for wavenumber in an infrared Fourier transform spectrometer) as long as their product is dimensionless.

The exponential in Eq. (2) can be expanded as

$$e^{i2\pi\nu t} = \cos(2\pi\nu t) + i \sin(2\pi\nu t) \tag{3}$$

to give

$$f(t) = \int_{-\infty}^{\infty} F(\nu) \cos(2\pi\nu t) d\nu + i \int_{-\infty}^{\infty} F(\nu) \sin(2\pi\nu t) d\nu. \tag{4}$$

The simple physical interpretation of Eq. (4) is that any arbitrary (not necessarily periodic) function $f(t)$ can be expanded as an integral ("sums") of sine and cosine functions, with $F(\nu)$ interpreted as the (complex) amplitudes of the "waves." The necessary amplitudes $F(\nu)$ can be obtained from Eq. (1), which thus represents the frequency analysis of the arbitrary function, $f(t)$. In other

☆*Change History*: September 2018. Peter F Bernath updated the previous article with a few minor editorial changes throughout the text. The main changes were in the Fourier Transform Applications section in which recent references were added and updates provided.

words, Eq. (1) analyses the function $f(t)$ in terms of its frequency components and Eq. (2) puts the components back together again to recreate the function. Notice that if $f(t)$ is an even function (i.e., $f(-t) = f(t)$), then the cosine transform suffices (i.e., only first term on the right hand side of (4) need be retained), but this is rarely the case in practice.

Fourier Transforms

The Fourier transform can be applied to a few simple functions as presented in pictoral form in Fig. 1. The Fourier transform of a Gaussian is another Gaussian, the decaying exponential (double-sided) gives a Lorentzian, and the boxcar function gives a sinc sin (x/x) function.

The Fourier transforms of a number of elementary functions require the use of the delta function, $\delta(v - v_0)$. The $\delta(v - v_0)$ function has the "sifting" property,

$$f(v_0) = \int_{-\infty}^{\infty} \delta(v - v_0) f(v) dv \tag{5}$$

that implies unit area,

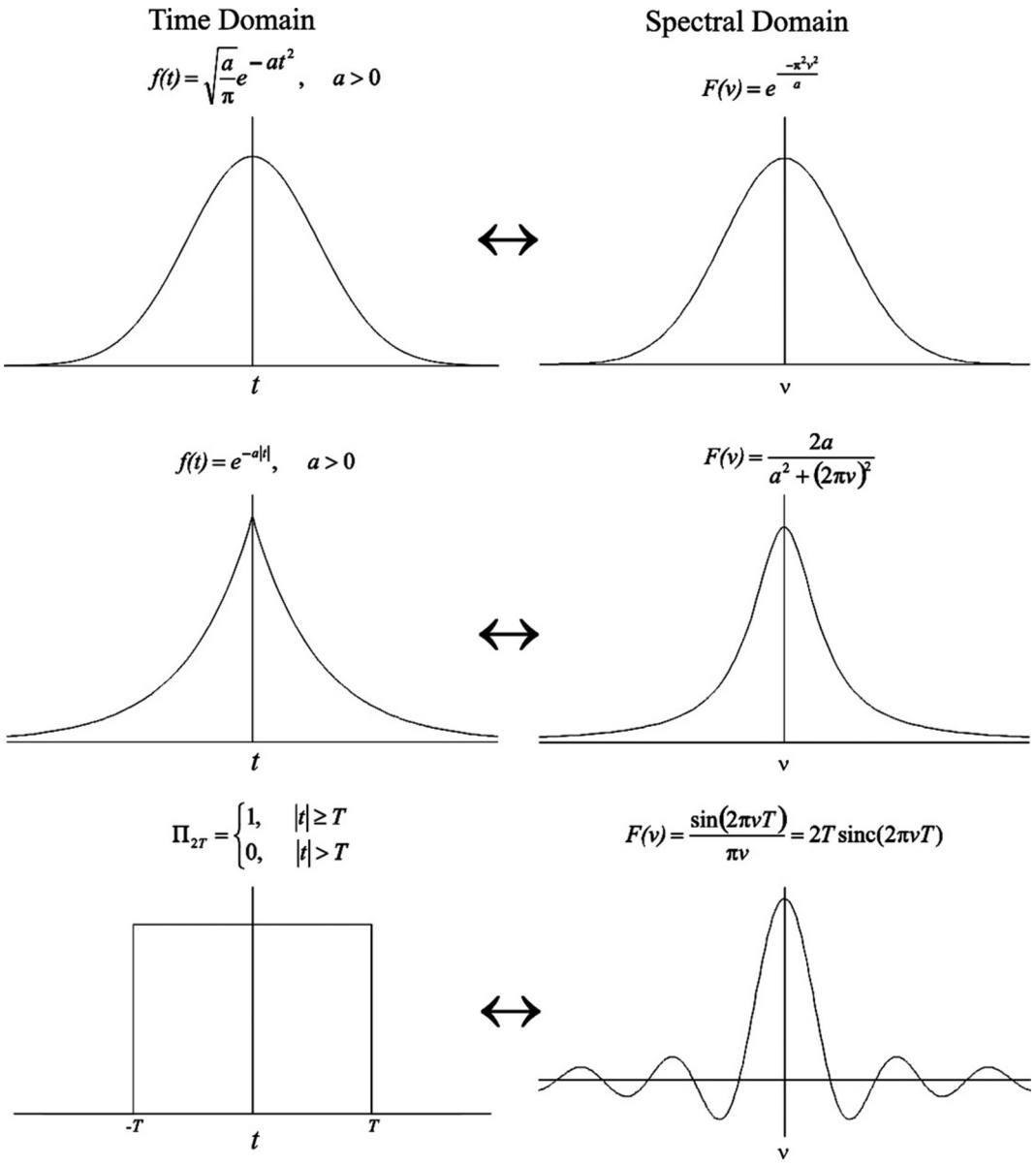

Fig. 1 The Fourier transforms of Gaussian, double-sided exponential and boxcar functions.

$$1 = \int_{-\infty}^{\infty} 1 \cdot \delta(v - v_0) dv \tag{6}$$

and a value of 0 for $v \neq v_0$.

The Fourier transform of the infinitely long wave, cos $(2\pi v_0 t)$, is thus, $(\delta(v - v_0) + \delta(v + v_0))/2$, which has a value of ∞ when $v = v_0$ and $v = -v_0$. The appearance of negative frequencies is at first surprising, but is required by the mathematics of complex numbers. The identity

$$\delta(v - v_0) = \int_{-\infty}^{\infty} e^{\pm i2\pi(v - v_0)t} dt \tag{7}$$

can be interpreted as the infinite sum of waves all phased to add up at $v = v_0$ and to cancel for $v \neq v_0$. No function in the usual sense can be infinitely high, infinitely narrow and still have unit area. In mathematics, the delta function is thus defined as the limit of a series of peaked functions such as Gaussians.

While the Fourier transform of the even cosine function is real, the result for sin $(2\pi v_0 t)$ is imaginary: $(\delta(v - v_0) + \delta(v + v_0))/(2i)$. Since the sine function is 90 degree out of phase to the corresponding cosine, it is clear that the imaginary axis is used to keep track of phase shifts, consistent with the polar representation of a complex number: $x + iy = re^{i\phi}$ with $r = \sqrt{x^2 + y^2}$ and $\phi = \tan^{-1}(y/x)$. In this phasor picture, positive and negative frequencies can be interpreted as clockwise and counter clockwise rotations in the complex plane.

The Fourier transform has many useful mathematical properties including linearity, and that the derivative $df(t)/dt$ has the transform $(i2\pi v)F(\nu)$. The convolution theorem is particularly useful because it relates the product of two functions, $F(v)$ G(ν), in the frequency domain to the convolution integral

$$f * g(t) \equiv \int_{-\infty}^{\infty} f(\tau) g(t - \tau) d\tau \tag{8}$$

in the time domain (or vice versa), using the upper case/lower case Fourier transform notation for the $(F(v), f(t))$, $(G(\nu), g(t))$ pairs. For example, a finite piece of a cosine wave represented by the product, cos $(2\pi v_0 t)\Pi_{2T}(t)$, leads to the convolution (Fig. 1) of two delta functions with a sinc function in the frequency domain. The result is, T sinc $(2\pi T(v - v_0)) + T$ sinc $(2\pi T(v + v_0))$, that is, the infinitely narrow δ-functions at $\pm\nu_0$ produced by the Fourier transform of the infinite cosine have been broadened into sinc functions for the more realistic case of a finite length cosine wave. Similarly, the Fourier transform of the double-sided decaying exponential wave, cos $(2\pi v_0 t)$exp. $(-a|t|)$, is two Lorentzians centered at $\pm v_0$ (Fig. 1) in the frequency domain.

Discrete Fourier Transform

The trouble with practical applications of Fourier's integral theorem is that it requires continuous functions for an infinite length of time. These conditions are clearly impossible so the case of a finite number of observations must be considered. Consider sampling the data every Δt for $2N$ equally-spaced points from $-N$ to $N-1$ with $t_j = j\Delta t$; $j = -N, -N+1, \ldots, 0, \ldots, N-1$. The Fourier transform, Eq. (1), then becomes the discrete Fourier transform:

$$F(v) = \Delta t \sum_{j=-N}^{N-1} f(j\Delta t) e^{-i2\pi v j} \Delta t. \tag{9}$$

The question immediately arises as to the number of points required to sample the signal $f(t)$. If not enough points are taken the signal will be distorted, and if too many points are used there is a waste of resources. The answer is a remarkable result due to Nyquist: given a signal with no frequency components above v_{max}, the signal can be completely recovered if it is sampled at a frequency of $2v_{max}$ (or greater). The Nyquist (or critical) sampling at $2v_{max}$ corresponds to two data points per wavelength for the frequency component at v_{max}. It seems almost magical that such sparse, minimal sampling allows exact recovery of the original signal by interpolation. The connection between the time and the frequency domains for critically sampled data is illustrated in Fig. 2. In the time domain, the interferogram is recorded from $-T$ to T with a point spacing $\Delta t = 1/(2v_{max})$, while in the spectral domain the data is present from $-v_{max}$ to v_{max} with a frequency point spacing of $\Delta v = 1/(2T)$. In the particular case of an even function, although $2N$ points $(2N = 2T/\Delta t = 2v_{max}/\Delta v)$ are displayed in Fig. 2, only N of them are independent. The discrete inverse Fourier transform is

$$f(t) = \Delta v \sum_{k=-N}^{N-1} F(k\Delta v) e^{i2\pi t k} \Delta v \tag{10}$$

with t only given at $t_j = j\Delta t$ in Eq. (10) and v given at $\nu_k = k\Delta\nu$ in Eq. (9).

Undersampling a signal is unfortunately a common occurrence and causes aliasing. A simple example of aliasing is the observation on television of a wheel on a wagon or a car rotating "backwards" as the vehicle moves forward. For older movies, motion picture cameras sample the image at 24 times per second (the frame rate) and the image of the rotating wheel is thus often

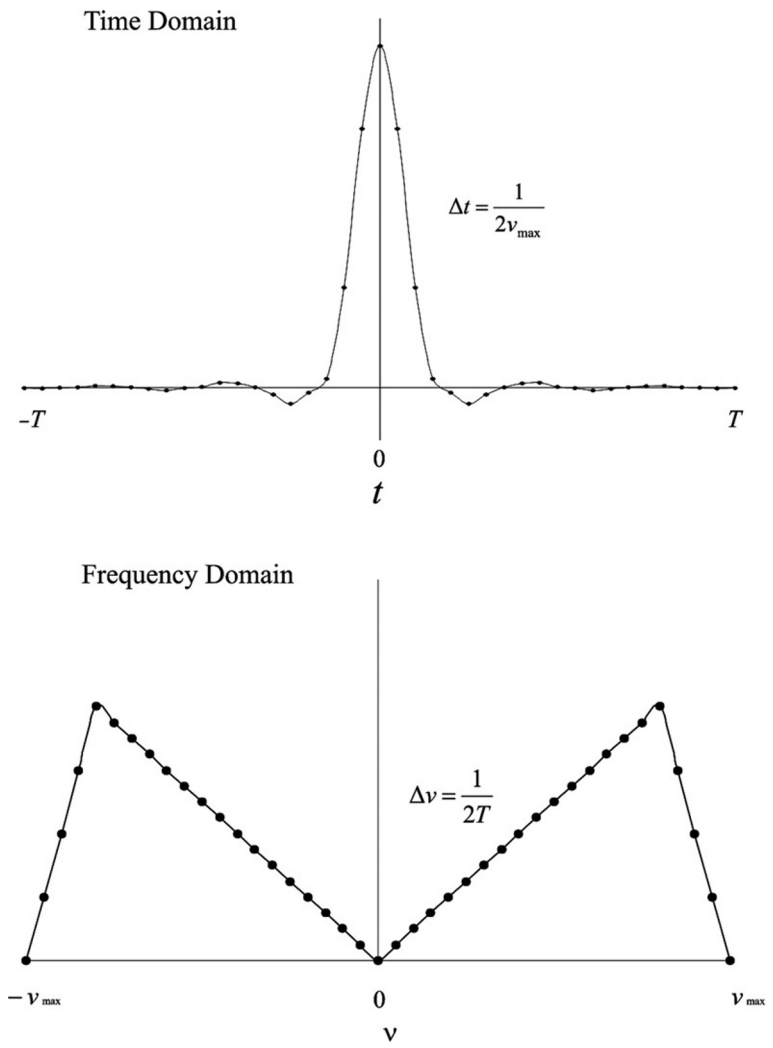

Fig. 2 Nyquist sampling in the spectral and time domains.

undersampled. When the sampling frequency ν_S is somewhat less than the required $2\nu_{max}$, then the spectrum between $\nu_S/2$ and ν_{max} is "folded back" about $\nu_S/2$ and appears as a reversed artifact between $-\nu_S/2$ and $\nu_S/2$. If the signal is very undersampled, then it can be folded (aliased) many times (like fan-folded printer paper) between $-\nu_S/2$ and $\nu_S/2$. This folding of the spectrum about $\nu_S/2$ is called aliasing.

Aliasing can sometimes be used to advantage. For example, if a spectrum has no signal between 0 and $\nu_{max}/2$, then every second point can be deleted ("decimation") because this undersampling by a factor of 2 will fold the signal from $\nu_{max}/2$ to ν_{max} backwards into the empty region from 0 to $\nu_{max}/2$.

The discrete Fourier transform, Eq. (9), can be evaluated in a brute force fashion on a computer using the available sine and cosine functions, Eq. (3), but this method is very slow for a large number of points. The Fourier transform algorithm of Cooley and Tukey is much faster. The derivation of the Cooley–Tukey algorithm ("fast Fourier transform") starts by rewriting the exponent in Eq. (10) as

$$i2\pi tk\Delta\nu = i2\pi j\Delta tk\Delta\nu = i\pi jk/N \tag{11}$$

using

$$t_j = j\Delta t; j = -N, \ldots, N-1 \text{ and } \Delta t\Delta\nu = \Delta t/(2T) = 1/(2N) \tag{12}$$

The discrete Fourier transform and inverse Fourier transform, Eqs. (9) and (10), thus become

$$F(\nu_k) = \Delta t \sum_{j=-N}^{N-1} f(j\Delta t) e^{-i\pi jk}/N = \Delta t \sum_{j=0}^{2N-1} f(j\Delta t) e^{-i\pi jk}/N \tag{13}$$

$$f(t_j) = \Delta \nu \sum_{k=-N}^{N-1} F(k\Delta \nu) e^{i\pi jk}/N = \Delta \nu \sum_{k=0}^{2N-1} F(k\Delta \nu) e^{i\pi jk}/N \tag{14}$$

and the limits of the summation are shifted from $-N$ to $N-1$ to 0 to $2N-1$ by considering the $f(t)$ from $-T$ to T and $F(\nu)$ from $-\nu_{max}$ to ν_{max} as periodic functions (Fig. 3). The fast Fourier transform requires $2N$ to be a power of two, that is, 2^m so the data are padded with zeros up to the next highest power of 2. The algorithm works by repeatedly (m times) dividing a $2N$-point transform into two smaller N-point transforms. The resulting final transform has $2N$ points in the frequency domain, with the first N covering 0 to ν_{max}. The second N points from ν_{max} to $2\nu_{max}$ are the aliased points from $-\nu_{max}$ to 0 (see Fig. 3).

The fast Fourier transform allows optimal interpolation of data. The original N points are folded about 0 to make $2N$ points and are then shifted by $+N$ (Fig. 3). The fast Fourier transform then creates $2N$ points in the frequency domain, which are padded by the desired number of extra zeros in the appropriate location in the middle (e.g., $6N$ zeros in total for fourfold interpolation) and transformed back. (The extra zeros are added in the middle because of the aliasing of points from $-\nu_{max}$ to 0 into ν_{max} to $2\nu_{max}$ as shown in Fig. 3). This procedure creates interpolated points between the original data points.

Fourier Transform Spectroscopy

Spectra are traditionally recorded by dispersing the radiation and measuring the absorption or emission, one point at a time. In some regions of the spectrum, for which tunable radiation sources are available, one can imagine stepping the frequency of the source from ν_n to ν_{n+1} by $\Delta\nu$ (Fig. 2) and recording the absorption. The primary attraction of Fourier transform techniques as

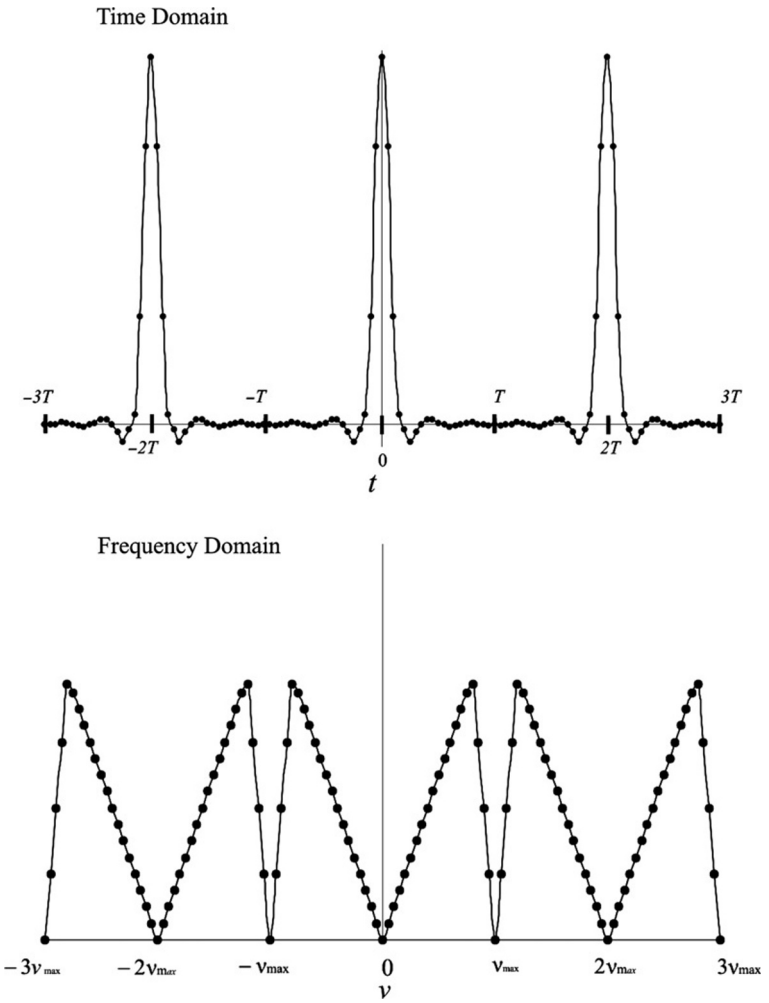

Fig. 3 Frequency and time domains with the signals considered to be periodic.

compared to the "traditional" approach is that all frequencies in the spectrum are detected at once. This property is the so-called multiplex or Fellgett advantage of Fourier transform spectroscopy.

Most Fourier transform measurements at long wavelengths (e.g., FT-NMR, Fourier Transform Nuclear Magnetic Resonance) are made by irradiating the system with a short broadband pulse capable of exciting all the frequency components of the system, and then monitoring the free induction decay response. Such an approach presumes the availability of a coherent, high power source of radiation that covers the entire spectral region of interest. A simple free induction decay has

$$f(t) = \mathrm{e}^{-at}\ \cos(2\pi\nu_0 t), t \geq 0, \mathrm{a} > 0$$

and

$$f(t) = 0, t < 0, \tag{15}$$

with the corresponding spectrum,

$$F(\nu) = \frac{1}{2(a + i2\pi(\nu - \nu_0))} + \frac{1}{2(a + i2\pi(\nu + \nu_0))} \tag{16}$$

If $\nu \approx \nu_0$ and $a \ll \nu_0$, then the second term of Eq. (16) can be dropped to give

$$F(\nu) = \frac{a}{2\left(a^2 + 4\pi^2(\nu - \nu_0)^2\right)} - \frac{i2\pi(\nu - \nu_0)}{2\left(a^2 + 4\pi^2(\nu - \nu_0)^2\right)}. \tag{17}$$

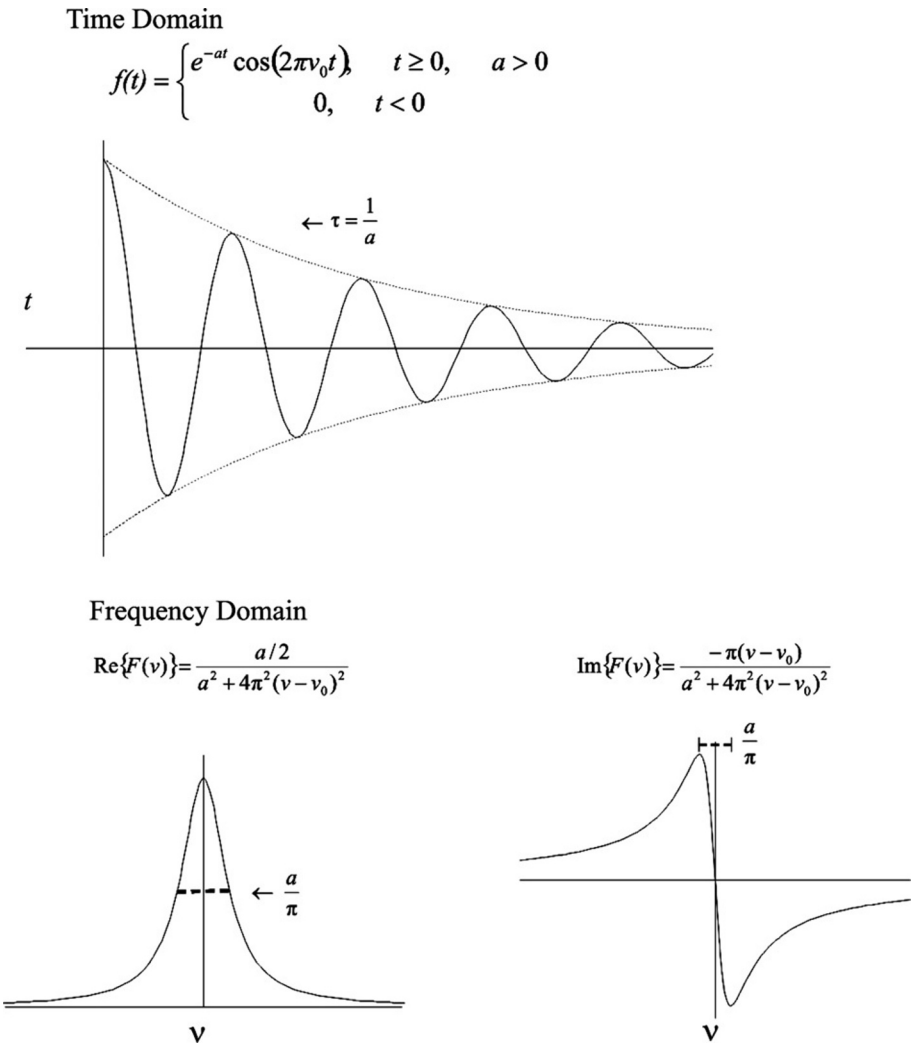

Fig. 4 Fourier transform of a free induction decay.

The real part of $F(v)$ is a Lorentzian centered at v_0 (first term on the right of Eq. 17), while the imaginary part (second term on the right of Eq. 17) is the corresponding dispersion curve (Fig. 4). The constant $1/a$ is the lifetime τ of the decay and the full width at half maximum of the Lorentzian is a/π.

As compared to a double-sided even function, it is the abrupt turn-on of the free induction decay at $t = 0$ that causes the large imaginary signal. All causal signals (defined to have $f(t) = 0$ for $t < 0$) have this property. The physical interpretation is that the abrupt start of the signal excites an in-phase response (the real part) to the cosine part of the original excitation wave as well as a response 90 degree out of phase (the imaginary part). The antisymmetric imaginary part is needed to cancel the symmetric real part for $t < 0$. The large imaginary frequency component means that typically the magnitude spectrum is computed as

$$|F(v)| = \sqrt{(\,\mathrm{Re}\,(F(v)))^2 + (\,\mathrm{Im}\,(F(v)))^2} \tag{18}$$

for practical applications in, for example, Fourier transform mass spectrometry.

As usual there is a reciprocal relationship between the time domain and the frequency domain. The more rapid is the damping (decay) of the signal (i.e., larger a and shorter lifetime $\tau = 1/a$), the wider the Lorentzian and dispersion lineshape functions become in the spectral domain (Fig. 4).

At higher frequencies, Fourier transform spectroscopy is generally carried out with a Michelson interferometer rather than by detection of a coherent transient decay. The Michelson interferometer divides the input radiation into two parts with a beamsplitter and then recombines them. As the optical path difference of the two parts is varied, the interference of the recombined beams produces an interferogram. If the optical path difference, x, changes at a constant rate, v, then the interferogram becomes a function of time, $f(x) = f(vt)$, and the Fourier transform yields the desired spectrum, $F(v)$. In general, double-sided interferograms are recorded from $-L$ $(= -vT)$ to $+L$ $(= vT)$ in optical path difference, as shown in Fig. 2. For practical reasons to save resources sometimes only a short double-sided interferogram is recorded to determine the phase. This low-resolution phase function is then interpolated to generate a high-resolution phase function and applied to a high-resolution single-sided spectrum recorded only from 0 to L, rather than from $-L$ to $+L$.

The main barrier to the use of free induction decay for Fourier transform spectroscopy in the infrared region is the lack of a convenient powerful source of broadband coherent radiation. In addition, the decay times for the coherently-excited polarization in the system tend to be very short at higher frequencies. Coherent terahertz spectrometers operating in the far infrared region are now practical because of the success of ultrafast laser technology in generating broadband terahertz pulses.

Fourier transform techniques are inherently digital and were not practical before the advent of the digital computer. The digital data can thus be filtered and manipulated with ease. In particular, the instrumental resolution can be varied at will and chosen to match the inherent resolution of the physical system. As shown in Fig. 2, recording the interferogram for a longer time T (longer optical path difference for a Michelson interferometer) results in a closer point spacing $\Delta v = 1/(2T)$ and higher instrumental resolution in the frequency domain. There are practical limits because when the interferometric signal is no longer visible because it is buried in noise, no further increase in resolution is possible. The Fourier transform spectrometer can thus easily trade decreased spectral resolution for increased signal-to-noise ratio. Very high instrumental resolutions are possible and resolving powers, $R \equiv v/\Delta v$, more than 10^6 can be achieved in the visible and infrared spectral regions, and for mass spectrometry.

When Fourier transform spectroscopy is implemented with a Michelson interferometer, there is an additional advantage over a grating or prism spectrograph that uses rectangular slits. The circular entrance aperture of the Michelson interferometer can be opened until the subtended solid angle, $\Omega_{\max}$, (in steradians, as measured using the distance to the collimator) is given by $R\Omega_{\max} = 2\pi$, with resolving power, R, computed for the highest measured frequency $v_{\max}$. For the same resolving power, a grating spectrograph typically has 50–100 times smaller $\Omega_{\max}$ as subtended by the slits. Much more radiation can thus enter the larger entrance aperture of a Fourier transform spectrometer than a grating spectrometer, as was first pointed out by Jacquinot. The throughput or Jacquinot advantage is always operative for a Michelson interferometer.

Surprisingly, the multiplex "advantage" of Fourier transform spectroscopy is not always available and depends on the principal noise source in the system. At low frequencies, the principal noise source is often detector or background noise. In this case, the noise is independent of the signal level and is constant. Compared to a single element detector used to detect a single frequency interval, Δv, the signal level for the Fourier transform spectrometer that detects N channels of width Δv is N times greater. The noise in these N channels also now appears at the detector, but because of partial cancellation due to the random nature of noise (mean value of zero), the noise level increases by only $\sqrt{N}$. Note that true noise always partially cancels in this manner but that signal artifacts ("periodic noise") will not generally do so. Overall then the signal-to-noise ratio has improved by $\sqrt{N}$ for a Fourier transform spectrometer.

To higher frequencies, in the visible region, photons carry more energy and can be detected, for example, by counting. The noise in such a system is typically due to "shot" noise arising from the Poisson statistics of random fluctuations in the arrival times of photons at the detector. Shot noise is proportional to the square root of the number of photons arriving at the detector. If the primary noise source is shot noise, then the noise is proportional to the square root of the signal level. In this case, for the N-channel Fourier transform spectrometer the signal level increases by N and the noise increases by $\sqrt{N}$ for the increased number of channels and another factor of $\sqrt{N}$ for the increased intensity. Overall there is no change in the signal-to-noise ratio as compared to a single channel spectrometer. Surprisingly then, in the visible region the multiplex advantage usually does not apply, although the throughput and "digital" advantages remain.

Unfortunately, there is a third possibility for the noise. In remote sensing applications in the Earth's atmosphere or in astronomy, the noise may be directly proportional to the signal level. Transmission through the atmosphere has random fluctuations ("scintillations") that are analogous to "$1/f$" noise that appears in electronic circuits at low frequency. In the laboratory, emission from a sample may be excited by a laser or other source that is plagued by amplitude fluctuations. There may also be a weak molecular emission of interest in a spectrum dominated by strong fluctuating lines from an extraneous atom or molecule. In all these cases, the N-channel Fourier transform spectrometer increases the signal by N over a single channel spectrometer, but the noise also increases by another factor of $\sqrt{N}$ for the increased number of channels and by N because of the increased intensity level. Incredibly, the signal-to-noise ratio has therefore decreased by $\sqrt{N}$ and there is a multiplex "disadvantage" for a Fourier transform spectrometer. Because the Fourier transform spectrometer detects all of the spectrum (including the noise) at one time, the noise from all of the channels is distributed throughout the spectrum. In a simple single channel spectrometer, only the noise from that single channel appears, even though nearby channels may have strongly fluctuating signals. It is this redistribution of noise from all channels that causes the Fourier disadvantage.

The presence of a multiplex disadvantage accounts for the enormous success of small multichannel visible spectrometers based on array detectors, as compared to low resolution visible Fourier transform spectrometers. In any case, for a specific application a careful analysis of the noise is indispensable for an optimum instrument.

Fourier Transform Applications

The Fourier transform technique has been applied in a multitude of different areas. Starting at low frequencies, Fourier transform (FT) methods have been used for dielectric response spectroscopy of solids (sometimes called time domain reflectometry). A short picosecond voltage pulse is applied to a dielectric and the current response is measured. Fourier transformation of the current gives the dielectric response function, $\varepsilon(\nu)$, which is typically interpreted as the Debye relaxation of dipoles.

The main application at low frequencies is, of course, nuclear magnetic resonance, NMR. In FT-NMR, a magnetized sample is irradiated by radio frequency (r.f.) radiation to manipulate the bulk magnetization. The basic signal is the free induction decay, but hundreds of sophisticated r.f. pulse sequences have been invented for specific purposes, including medical imaging.

A related r.f. technique to NMR is nuclear quadrupole resonance, NQR. In NQR, transitions between nuclear quadrupole levels of nuclei in a solid material are induced by the applied radiation. The electric field gradients in the solid orient the quadrupolar nuclei ($I > 1/2$) and give rise to quantized energy levels that yield transitions in the MHz range. FT-NQR spectroscopy measures these splittings and the relaxation times by free induction decay or various pulse echo experiments. FT-NQR spectroscopy provides information about the local environment around the quadrupolar nucleus in a crystal.

Electron spin resonance, ESR, operates at somewhat higher frequencies in the GHz range and is sometimes called electron paramagnetic resonance, EPR. ESR is like NMR but uses electron spins rather than nuclear spins. By definition, FT-ESR studies free radicals, and it is more sensitive than FT-NMR but of less general applicability. Related to ESR is muon spin resonance (μSR), carried out at high energy accelerator sources such as TRIUMF (Vancouver, Canada) that provide muons.

In the gigahertz region, Fourier transform microwave (FT-microwave) experiments were pioneered by the late W.H. Flygare. FT-microwave experiments use a short pulse of microwave radiation to polarize a gaseous sample in a waveguide or, more commonly, in a Fabry–Perot cavity. Free induction decay is detected and Fourier transformed into a spectrum. FT-microwave spectroscopy of cold molecules in pulsed jet expansion is particularly popular because of the increased sensitivity associated with low temperatures, and the possibility of studying large molecules and van der Waals complexes. More recently B. Pate has developed the technique of chirped pulse Fourier transform microwave spectroscopy (CP-FTMW) in which a frequency-swept pulse of microwave radiation polarizes the sample over a broad frequency range and all of the free induction decays are measured simultaneously with a fast oscilloscope.[6]

In the infrared, visible and near ultraviolet regions, Fourier transform methods generally use the Michelson interferometer rather than detecting a free induction decay. Originally instruments were custom built, for example, by P. and J. Connes in France and J. Brault in the United States, but commercial instruments now dominate except for a few special applications. The short wavelength limit for the Michelson interferometer has been extended to 40 nm in the vacuum ultraviolet region for use with the SOLEIL synchrotron.[4] The use of synchrotron radiation as a source of radiation for high resolution far infrared FTS spectroscopy has expanded greatly.[5] Imaging FTS instruments are now commercially available. Recently, coherent time domain terahertz spectroscopy has become possible in the far infrared region. In this case, the system is polarized with an ultrashort pulse of terahertz radiation and the coherent decay is detected using ultrafast laser techniques.[1] Dual comb spectroscopy using frequency combs from two ultrafast lasers has emerged as a promising FTS technique.[3] FTS applications in infrared remote sensing have proliferated from ground-based, airborne and satellite platforms; for example, the Atmospheric Chemistry Experiment Fourier Transform Spectrometer (ACE-FTS) is making Earth observations using the Sun as a light source.[2]

Fourier transform techniques have also been applied with great success to mass spectrometry. The ion cyclotron resonance (ICR) spectrometer traps ions in a magnetic field. The ions travel in circles about the applied magnetic field (cyclotron motion) and are trapped in the direction along the magnetic field by small voltages applied to the end caps of the trapping cell. A short pulse of r.f. radiation coherently phases the ions in the trap and increases their orbits. The phase coherent orbiting ions induce small image currents on the two opposite walls of the trapping cell. The Fourier transform of these image currents yields the mass spectrum. In this case, the decay time of the free induction decay signal can be very long because the dephasing of the cyclotron motion of the ions in a homogenous magnetic field is controlled by collisions with residual gas. The FT-ICR technique can thus have ultrahigh mass resolution and great sensitivity.

References

1. Beard, M. C.; Turner, G. M.; Schmuttenmaer, C. A. Terahertz Spectroscopy. *J. Phys. Chem. B* **2002**, *106*, 7146–7159.
2. Bernath, P. F. The Atmospheric Chemistry Experiment (ACE). *J. Quant. Spectrosc. Radiat. Transfer* **2017**, *186*, 3–16.
3. Coddington, I.; Newbury, N.; Swann, W. Dual-Comb Spectroscopy. *Optica* **2016**, *3*, 414–426.
4. de Oliveira, N.; Roudjane, M.; Joyeux, D.; et al. High-Resolution Broad-Bandwidth Fourier-Transform Absorption Spectroscopy in the VUV Range down to 40 nm. *Nat. Photonics* **2011**, *5*, 149–153.
5. McKellar, A. R. W. High-Resolution Infrared Spectroscopy With Synchrotron Sources. *J. Mol. Spectrosc.* **2010**, *262*, 1–10.
6. Park, G. B.; Field, R. W. Perspective: The First Ten Years of Broadband Chirped Pulse Fourier Transform Microwave Spectroscopy. *J. Chem. Phys.* **2016**, *144. 200901*.

Further Reading

Bell, R. J. *Introductory Fourier Transform Spectroscopy*; Academic Press: New York, 1972.
Bracewell, R. N. *The Fourier Transform and Its Applications*, 3rd ed; McGraw-Hill: New York, 2000.
Brigham, E. *Fast Fourier Transform and Its Applications*; Prentice Hall: Englewood Cliffs, NJ, 1988.
Chamberlain, J. *The Principles of Interferometric Spectroscopy*; Wiley-Interscience: Chichester, 1979.
Davis, S.; Abrams, M. C.; Brault, J. M. *Fourier Transform Spectrometry*; Academic Press: San Diego, 2001.
Griffiths, P. R.; De Haseth, J. A. *Fourier Transform Infrared Spectrometry*; 2nd ed; Wiley-Interscience: Hoboken, NJ, 2007.
Kauppinen, J.; Partanen, J. *Fourier Transforms in Spectroscopy*; Wiley-VCH: Berlin, 2001.
Lathi, B. P. *Communication Systems*; Wiley: New York, 1968.
Marshall, A. G., Ed.; In *Fourier, Hadamard, and Hilbert Transforms in Chemistry*; Plenum: New York, 1982.
Marshall, A. G.; Verdun, F. R. *Fourier Transforms in NMR, Optical, and Mass Spectrometry: A User's Handbook*; Elsevier: Amsterdam, 1990.
Schweiger, A.; Ieschke, G. *Principles of Pulse Electron Paramagnetic Resonance*; Oxford University Press: New York, 2001.
Slichter, C. P. *Principles of Magnetic Resonance*, 3rd ed; Springer: Berlin, 1992.
Thorne, A.; Litzen, U.; Johansson, S. *Spectrophysics*; Springer: Berlin, 1999.